

PAPER • OPEN ACCESS

Research on Seismic Behavior of Beam-Column Joints of New Prefabricated Steel Structure

To cite this article: Ni Zhandong 2020 *IOP Conf. Ser.: Earth Environ. Sci.* **560** 012010

View the [article online](#) for updates and enhancements.

You may also like

- [Cyclic load Analysis of beam column joint using ANSYS](#)
Pranali Wasnik, Prof. Sanket Sanghai and P.Y. Pawade
- [Numerical simulations of the bond stress-slip effect of reinforced concrete on the push over behavior of interior beam-column joint](#)
Sudarno P Tampubolon, Chung-Yue Wang and Ren-Zuo Wang
- [Research on Design and Construction Technology of Laminated Prefabricated Beam-column Joints](#)
Han Shangyu, Chen Jiashen, Yan Hao et al.



ECS
The
Electrochemical
Society
Advancing solid state &
electrochemical science & technology

DISCOVER
how sustainability
intersects with
electrochemistry & solid
state science research

Research on Seismic Behavior of Beam-Column Joints of New Prefabricated Steel Structure

Ni Zhandong*

Taizhou vocational and technical college, Taizhou, 318000, China

*Corresponding Author's E-mail: yixiao_5752@qq.com

Abstract. The advancement of technology has changed the function and structure of the building space. The prefabricated steel structure is in a period of vigorous development, which is an important way for the development of industrialization of buildings. Therefore, the key technology of prefabricated assembled steel structure is a key problem that needs to be solved urgently. It is particularly important in the optimization and upgrading of the form of the building structure. At the same time, the design and construction of the beam-column connection node is also crucial, which directly affects the construction process and speed. In this paper, a new type of assembled steel structure beam-column joint is designed, and the seismic behavior of the structure is analyzed through experiments. Experiments show that the structure has good seismic behavior, which not only effectively solves the problem of structural interference, but also reduces the construction process and improves the construction speed.

1. Introduction

The construction industry has a long history in China. Since the founding of New China, the construction industry has played a very important role in promoting China's economic and social development. However, there are still many problems in China's construction industry. For example, the energy consumption generated by the construction industry and related industries is very high, accounting for more than 30% of the total energy consumption of the society. Traditional construction operations will produce a lot of pollution, such as noise pollution, dust pollution, environmental problems are very serious. At the same time, it causes a lot of waste of hydropower resources [1]. These phenomena do not conform to the strategic policy of sustainable development. At present, the aging problem of the Chinese population is already very serious. The young labor force is declining year by year, and the population advantage no longer exists [2]. The cost of labor is gradually rising, which shows that the construction industry's inefficient and extensive building construction model is bound to be eliminated [3].

In view of the problems existing in the traditional construction model, after several years of research, it was found that industrialization of construction is one of the ways to solve the problem. In recent years, the country has vigorously promoted the industrialization of construction. Prefabricated steel frame structures are one of the ways of industrialized construction. Assembled steel frame structure refers to processing and manufacturing in the factory, and then transported to the site by means of transportation to assemble the components together with reliable connection. Reduced the number of workers required on site, while reducing on-site operations, which is conducive to achieving the green development requirements of environmental protection [4].



2. Design of test piece and loading scheme

The connection method of prefabricated steel structure beam-column nodes is different, the energy dissipation mechanism is different, and the seismic behavior of the node is related to the seismic capacity of the entire frame structure [5]. Therefore, it is very important to study the seismic behavior of new prefabricated steel beam-column joints. In this paper, the beam pre-assembled frame beam-column joints are subjected to a low-circumferential repositioning and loading test at the beam end, and the destruction forms of the joints are observed.

2.1 Specimen design

In this paper, according to GB50017-2017 "Steel Structure Design Standards" and JGJ101-2015, Two 1:1 T-shaped steel connection steel frame mid-span test specimens JD1 and JD2 with different thicknesses were produced [6]. The specific dimensions of the experimental model are shown in Table 1. The test pieces are all made of H-shaped steel, and the height of the column part of the node is taken between the reverse bending points of the upper and lower two-layer columns, and the height is 3.12m. Researchers take two sections of beams at the inflection points on both sides of the column, each section of the beam is 1.8m long. The beams and columns are connected by split T-shaped steel connectors, the bolt type is M10 type 10.9 bolts, and the bolt hole diameter is 23.5mm. A total of 32 bolts are used. High-strength bolts use a torque wrench to apply a preload of 190kN to the high-strength bolts in accordance with JGJ82-2011 "Technical Specifications for High-Strength Bolt Connections in Steel Structures". The nodes are shown in Figure 1.

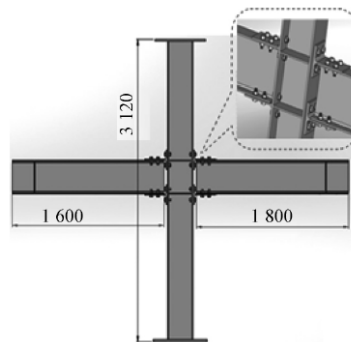


Figure 1. Test Piece

The specific dimensions are shown in Table 2. The elastic modulus of beams, columns and T-beams is 215GPa, and the Poisson's ratio is 0.3. All friction is set to contact, defined as Penalty, and the coefficient of friction is 0.3. The bolt hole and bolt diameter are both 22 mm, and there is no gap between the bolt and bolt hole.

Table1. Main parameters of the two test pieces

node	Column section	Height	Length	Beam section	T-section cross-section	Height
JD1	300×300×10×15	3 120	1 800	35×175×7×11	446×199×8×12	270
JD2	300×300×10×15	3 120	1 800	35×175×7×11	446×199×10×116	270

2.2 Loading scheme

The test adopts pseudo-static test, and the design load is shown in Table 2. Use the jack to apply the vertical load until it reaches the design value and keep it unchanged. In this process, ensure that the beam end sensor shows zero. The horizontal load is applied by the actuator, and the test horizontal load is divided into two stages of force control and displacement control. According to the estimated yield load, the force control method is adopted, and the load is divided into three levels before the yield load, and each level is cycled once. After yielding, load is controlled according to displacement [7]. The

displacement increment is 0.5 times the yield displacement, and each displacement cycle is repeated twice until the specimen fails. See Table 2 for the formal loading system.

Table 2. load loading system

Loading step	Load N/kN	Counterweight	Horizontal actuator	Cycles
Force control	1		20	
	2		40	
	3	Hanging basket 71kg	60	F-mean cycle once
...	80	
Displacement control	5	500 Counterweight 160kg		
	8	500 Hanging basket 71kg		F-mean cycle once
	9	Counterweight 160kg		

3. Analysis of experimental results

The strength, stiffness, ductility, energy consumption and other characteristics of the component can be learned through the skeleton curve of each node, and the seismic behavior of the component can be qualitatively compared and measured, which is also an important basis for determining the characteristic points in the resilience model.

3.1 Hysteresis Behavior

The hysteresis curve is the load-deformation curve of a structure or member under repeated loads. It reflects the characteristics of the structure's deformation, stiffness degradation, strength degradation, or energy consumption during repeated loading. It is a model for determining the resilience and nonlinear earthquakes [8]. Basis for reaction analysis.

The hysteretic curves of JD1 and JD2 nodes are Fig. a and b in Figure 2 respectively. It can be seen by comparing the curves: the hysteresis curve of JD2 is fuller than that of JD1, and the hysteresis loop of JD2 is larger than that of JD1, indicating that the ductility and energy dissipation capacity of JD2 is stronger than that of JD1. The positive yield bearing capacity of the JD1 specimen is 185.83kN, the negative yield bearing capacity is -186.18kN, the positive yield bearing capacity of the JD2 specimen is 295.83kN, and the negative yield bearing capacity is -287.18kN. The positive and negative yield bearing capacity of JD2 has been greatly improved, indicating that increasing the thickness of the web and flange of the T-shaped steel connector can improve the bearing capacity of the node. Figure 3 is a comparison of the skeleton curves of JD1 and JD2. At the beginning of loading, the load-displacement curve is linearly distributed, indicating that the node is in the elastic stage. After the node reaches yield, the load-displacement curve shows a non-linear distribution, and the load increases slowly, indicating that the node has entered plastic deformation at this time [9].

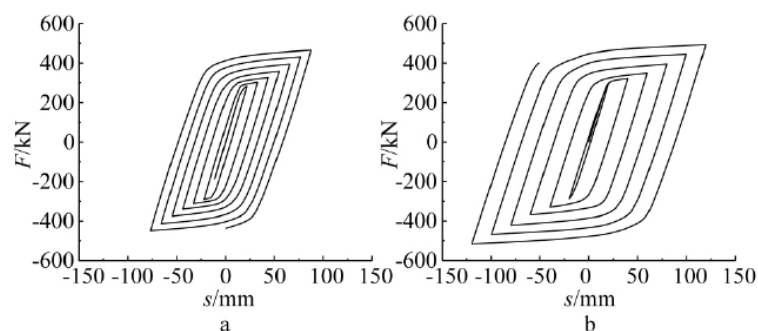


Figure 2. Hysteresis Curve

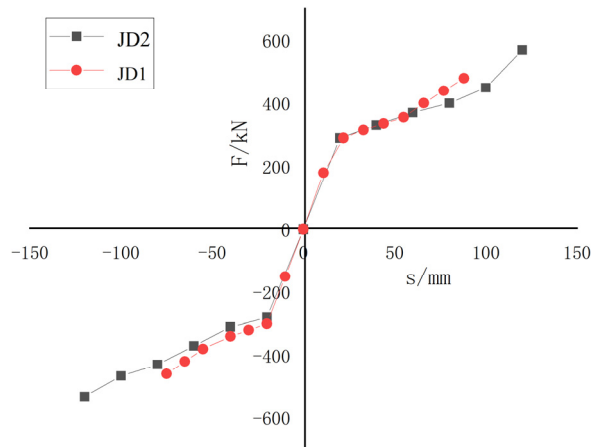


Figure 3. Skeleton curve

3.2 Degradation of strength and stiffness of specimen

Strength degradation refers to the fact that when the displacement amplitude remains unchanged, and the bearing capacity of the member decreases with the increase of the number of cyclic loads. In order to reveal the strength degradation law of the node under the external force, this paper analyzes the bearing capacity degradation of each cycle under the same level loading, and compares with the bearing capacity reduction coefficient λ_n , which is calculated as follows.

$$\lambda_n = \frac{F_m^n}{F_m^{n-1}} \tag{1}$$

F_m^n is the peak load value of the nth cycle when the displacement ductility coefficient is m . F_m^{n-1} is the peak load value of one less than the nth cycle when the displacement ductility coefficient is m . As shown in Figure 4, the number of load cycles is represented by the abscissa, and the ordinate represents the ratio of maximum bearing capacity of the test specimen per cycle to the bearing capacity of the previous cycle. From Fig. 4, We can know that the specimens all show a clear strengthening section after yielding. JD2 has changed significantly, which is due to the failure of the test piece in the middle of the test and the continued loading after the reinforcement. The strength degradation performance of JD1 is relatively stable, indicating that increasing the shaft pressure ratio at a certain axial pressure ratio improves the strength degradation performance [10].

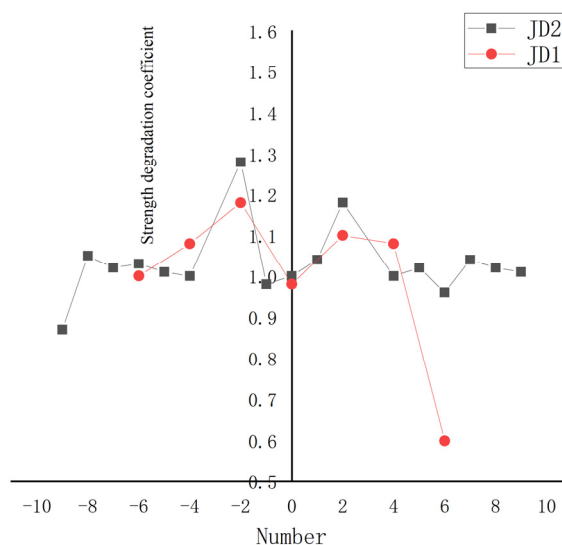


Figure 4. Strength degradation curve

In the repeated load test of the joints, the secant stiffness is used to evaluate the stiffness changes of the joints and then the cumulative damage of the structure. During the loading process of the specimen, the attenuation curve of secant stiffness with the number of cumulative loads is shown in Figure 4. The abscissa represents the cumulative number of cycles, and the ordinate represents the secant stiffness, as in Equation 2.

$$K_i = \frac{|-F_i| + |F_i|}{|-\delta_i| + |\delta_i|} \quad (2)$$

$+F_i$ and $-F_i$ are the peak loads of the i th cycle in the push and pull directions, respectively; $+\delta_i$ and $-\delta_i$ are displacements corresponding to $+F_i$ and $-F_i$.

It can be seen from Figure 5: Before 3 times the yield displacement, the stiffness of the two models JD1 and JD2 decreases relatively fast. After 3 times the yield displacement, the stiffness decline becomes gentle. The main reason for this phenomenon: before 3 times the yield displacement, there is slippage between the bolt rod and the bolt hole. The initial stiffness of JD2 is 16.27% higher than that of JD1. The stiffness of JD2 at 4 times the yield displacement is increased by 32.9% compared to JD1. The stiffness of JD2 at 6 times yield displacement is increased by 31.5% over JD1, indicating that increasing the thickness of the T-shaped steel can enhance the stiffness of the joint.

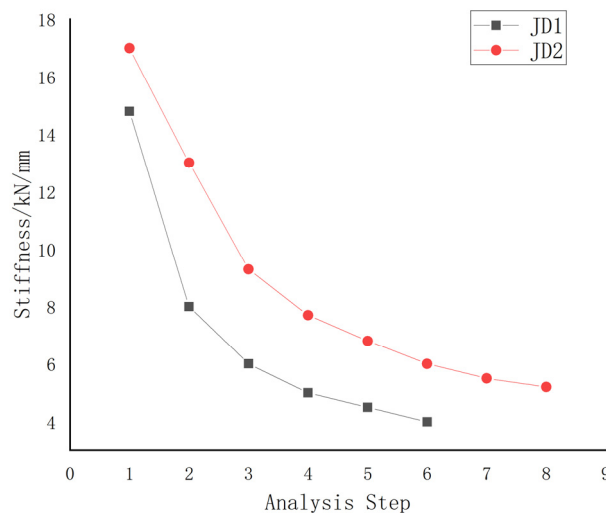


Figure 5. Stiffness degradation curve

3.3 Energy consumption and Ductility

Energy consumption and ductility are two important indicators of seismic behavior. Ductility is usually expressed by the ductility μ coefficient. The larger the value of μ , the better the node ductility. According to the provisions of JGJ/T 101-2015, the ductility coefficient of a node refers to the ratio of the limit displacement to the yield displacement, that is as follow.

$$\mu = \frac{\Delta x}{\Delta y} \quad (3)$$

Δy is the yield displacement, and Δx is the displacement corresponding to the limit load point.

When measuring the energy dissipation capacity of the test piece, it can be measured by the area enclosed by the hysteresis curve, and it is expressed by the equivalent damping viscosity coefficient h_e or the energy dissipation coefficient E . The value is larger, the energy dissipation ability is stronger. Here, the energy dissipation coefficient corresponding to its limit load is taken.

The analysis and test results show that the interlayer displacement ductility coefficient of the two specimens in this test is $\mu=2\sim 2.66$, both of which are greater than 2. The equivalent viscous damping coefficient $h_e = 0.287\sim 0.45$, the node has good energy dissipation capacity.

Table 3. Ductility and energy consumption indicators

Specimen	μ	φ_y	φ_y/θ_c	φ_u	φ_u/θ_p	θ_u	E	h_c
JD1	2.42	0.0326	8.17	0.079	3.96	0.078	2.342	0.372
JD2	2.67	0.0272	6.79	0.072	3.62	0.071	2.824	0.45

4. Conclusion

Through the discussion in this article, it shows that the change in the length of the embedded steel in the beam has no obvious effect on the degradation of the bearing capacity of the new type of prefabricated beam-column joints and the energy dissipation coefficient. The length of the embedded steel in the beam has a great influence on the stiffness and ductility of the joint members. The analysis results show that the embedded steel in the beam needs to meet the minimum length requirement, otherwise the node stiffness and ductility will decrease significantly.

The new prefabricated steel structure node can achieve construction requirements such as full bolting on the site, self-reset after earthquake, damage control and performance-oriented seismic design goals. At this stage, the damage-controlled prefabricated steel structure node is more suitable for popularization and application than self-reset node. The installation and operation space of prefabricated steel supports is also relatively large, and the construction is convenient. Therefore, the seismic design of the fabricated steel structure should be implemented in the manner of “first relying on the support and then the nodes”. It is necessary to promote the formation of assembly steel structure design and construction specifications, and apply some of the relatively mature assembly steel structure seismic components, components and corresponding design methods to build typical demonstration projects to promote the popularization and application of assembly steel structures.

References

- [1] Ha S S and Kim S H. 2014 Performance Evaluation of Semi Precast Concrete Beam-Column Connections with U-Shaped Strands. *Advances in Structural Engineering*, vol 17, pp 1585-1600.
- [2] Li H. 2015 Research on the Development Trend of Welding Technology for Building Steel Structure. *Shanxi Architecture*, vol 25, pp 108-111.
- [3] Mou B, Pang L Y, Qiao Q Y, et al. 2018 Experimental investigation of unequal-depth-beam-to-column joints with t-shape connector. *Engineering Structures*, vol 174, pp 663-674.
- [4] Wei B, Zhou X Q, Min B, et al. 2016 Research on Mechanical Performance of High-strength Bolt of Tension T-connector. *Journal of Building Structure*, pp 380-387.
- [5] Mou M, Wang L L, Zhang C W, et al. 2018 Seismic Performance of Outer ring-plate beam-column Joints Considering the Effect of Floor Slab: Experimental Study. *Engineering Mechanics*, vol 2, pp 160-168+213.
- [6] Wang Z. 2013 Finite Element Numerical Simulation of Steel Structure Bolt Connection. *Low Temperature Architecture Technology*, vol 35, pp 61-63.
- [7] Shahabeddin T, Seyed R M, Farhad K. 2012 Moment connection between I beam and built up square column by a diagonal through plate. *Journal of Construction steel Research*, 70: 385-401.
- [8] Parastesh H, Hajirasouliha I, Ramezani R. 2014 A new ductile moment-resisting connection for precast concrete frames in seismic regions: An experimental investigation. *Engineering Structures*, 70: 144-157.
- [9] Shan Q F. 2016 Optimum design and seismic performance of beam-column joints in fabricated frame structures. Nanjing: Southeast University.
- [10] Du K C. 2017 Research on mechanical properties of reinforced concrete prefabricated beam-column member I-beam connection. Harbin: Harbin Institute of Technology.